Normative Aortic Valvar Measurements in Adults Using Cardiac Computed Tomography — A Potential Guide to Further Sophisticate Aortic Valve-Sparing Surgery —

Izawa, Yu ; Mori, Shunpei ; Tretter, T., Justin ; Quintessenza, A., James ; Toh, Hiroyuki ; Toba, Takayoshi ; Watanabe, Yoshiaki ; Kono,…

(Citation)
Circulation Journal,85(7):CJ-20-0938

(Issue Date)
2021-01-07

(Resource Type)
journal article

(Version)
Version of Record

(URL)
https://hdl.handle.net/20.500.14094/90009366

Circulation Journal
Circ J 2021; 85: 1059–1067
doi:10.1253/circj.CJ-20-0938

ORIGINAL ARTICLE
Imaging

Normative Aortic Valvar Measurements in Adults Using Cardiac Computed Tomography
— A Potential Guide to Further Sophisticate Aortic Valve-Sparing Surgery —

Yu Izawa, MD; Shumpei Mori, MD, PhD; Justin T. Tretter, MD; James A. Quintessenza, MD; Hiroyuki Toh, MD; Takayoshi Toba, MD, PhD; Yoshiaki Watanabe, MD, PhD; Atsushi K. Kono, MD, PhD; Kenji Okada, MD, PhD; Ken-ichi Hirata, MD, PhD

Background: A thorough understanding of the anatomy of the aortic valve is necessary for aortic valve-sparing surgery. Normal valvar dimensions and their relationships in the living heart, however, have yet to be fully investigated in a 3-dimensional fashion.

Methods and Results: In total, 123 consecutive patients (66±12 years, Men 63%) who underwent coronary computed tomographic angiography were enrolled. Mid-diastolic morphology of the aortic roots, including height of the interleaflet triangles, geometric height, free margin length of each leaflet, effective height, and coaptation length were measured using multiplanar reconstruction images. Average height of the interleaflet triangle, geometric height, free margin length, effective height, and the coaptation length were 17.3±1.8, 14.7±1.3, 32.6±3.6, 8.6±1.4, and 3.2±0.8 mm, respectively. The right coronary aortic leaflet displayed the longest free margin length and shortest geometric height. Geometric height, free margin length, and effective height showed positive correlations with aortic root dimensions. Coaptation length, however, remained constant regardless of aortic root dimensions.

Conclusions: Diversities, as well as characteristic relationships among each value involving the aortic root, were identified using living-heart datasets. The aortic leaflets demonstrated compensatory elongation along with aortic root dilatation to maintain constant coaptation length. These measurements will serve as the standard value for revealing the underlying mechanism of aortic regurgitation to plan optimal aortic valve-sparing surgery.

Key Words: Anatomy; Aortic root; Aortic valve, repair; Computed tomography

Aortic valve-sparing surgery has become one of the popular operational options for the primarily regurgitant valve and/or proximal aortic aneurysm over the last few decades.[1–5] Although outcomes of aortic valve-sparing surgery have improved,[6–8] there remain problems, including intraoperative conversion to aortic valve replacement or recurrence of aortic regurgitation.[9–11] As the aortic root anatomy is too complicated to accurately evaluate only with 2-dimensional methodology,[2,12,13] 3-dimensional evaluation is necessary to reveal the underlying mechanism of the aortic regurgitation and to define the predictors of successful surgical repair.[11,12,14] However, few quantitative data on the repair-oriented 3-dimensional anatomy of the aortic root are currently available, which impairs standardization of the surgical technique.[1,11] The aim of the present study is to measure the precise metrics of the normal aortic valve as the standard value for guiding successful surgical repair by using computed tomography.[15]

Methods

Study Population

We retrospectively analyzed the datasets obtained from 264 consecutive patients who underwent cardiac computed

Received September 10, 2020; revised manuscript received October 6, 2020; accepted October 10, 2020; J-STAGE Advance Publication released online January 7, 2021 Time for primary review: 10 days
Division of Cardiovascular Medicine, Department of Internal Medicine (Y.I., S.M., H.T., T.T., K.H.), Department of Radiology (Y.W., A.K.K.), Department of Cardiovascular Surgery (K.O.), Kobe University Graduate School of Medicine, Kobe, Japan; The Heart Institute, Cincinnati Children's Hospital Medical Center, Cincinnati, OH (J.T.T., J.A.Q.); Department of Pediatrics, University of Cincinnati College of Medicine, Cincinnati, OH (J.T.T.); and Kentucky Children's Hospital, University of Kentucky, UK Healthcare, Lexington, KY (J.A.Q.), USA
Mailing address: Shumpei Mori, MD, PhD, Division of Cardiovascular Medicine, Department of Internal Medicine, Kobe University Graduate School of Medicine, 7-5-1 Kusunoki-cho, Chuo-ku, Kobe 650-0017, Japan. E-mail: Shumpei_8@hotmail.com

ISSN-1346-9843

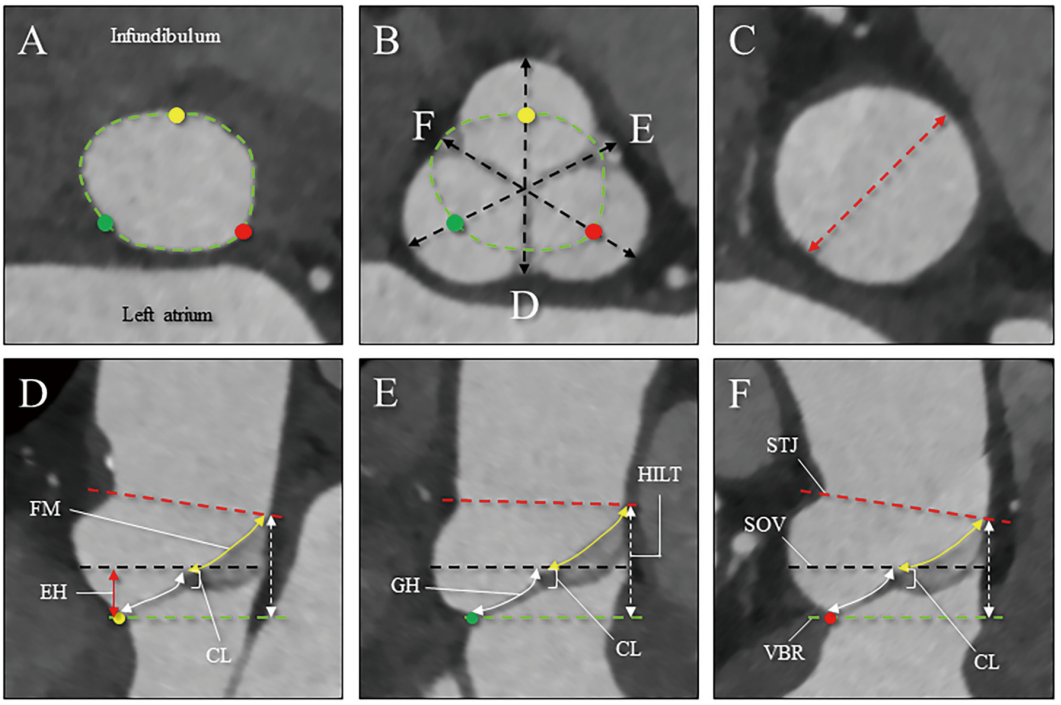

Figure 1. Measurements of the aortic root and aortic valve. (**A**) The virtual basal ring plane (yellow-green dashed line). (**B**) The sinuses of Valsalva plane at the level of the central coaptation point of the three aortic leaflets. Sections indicated by black dashed double-head arrows (**D**–**F**) correspond to the sections presented in lower panels. The virtual basal ring is precisely projected in this image. (**C**) The sinutubular junction plane. Red dashed double-head arrow indicates maximal short axis diameter. (**D**–**F**) Each bisecting plane. Yellow-green, black, and red dashed lines represent the virtual basal ring, sinuses of Valsalva, and sinutubular junction planes, respectively. White dashed double-head arrows represent the heights of the interleaflet triangles. White double-head arrows indicate the geometric heights. Yellow double-head arrows denote free margin lengths. The effective height (red double-head arrow) represents the vertical distance between the virtual basal ring and the sinuses of Valsalva plane cut at the top of the central zone of coaptation. The coaptation length was defined as the distance of central coaptation of the leaflets. Yellow, red, and green circles indicate the three nadirs of the hingelines of the right, left, and non-coronary aortic leaflets, respectively. CL, coaptation length; EH, effective height; FM, free margin; GH, geometric height; HILT, height of the interleaflet triangle; SOV, sinuses of Valsalva; STJ, sinutubular junction; VBR, virtual basal ring.

tomography from June 2017 to May 2018 at Kobe University Hospital. We excluded the following cases: moderate to severe aortic stenosis (n=73); moderate to severe aortic regurgitation (n=3); a history of surgery to the aortic valve (n=24); ascending aortic disease (n=9); a history of surgery for congenital heart disease (n=5); or inappropriate phase data acquisition (n=27). As a result, 123 patients with a structurally and functionally normal aortic valve with normal size aortic roots were included in the analyses. This study was conducted in accordance with the Declaration of Helsinki and was approved by the institutional ethical committee. Informed consent was obtained in the form of opt-out on the website.

Image Acquisitions

All acquisitions were performed using a third-generation dual-source computed tomographic scanner (SOMATOM Force; Siemens Healthcare, Forchheim, Germany). We used a standard protocol of prospective or retrospective electrocardiographically gated coronary arterial computed tomographic angiography. All images were acquired during a deep inspiratory breath-hold, using the parameters of tube voltage of 70–120 kV, tube current modulated with an automated exposure control, a gantry rotation of 250 ms, and a temporal resolution of 66 ms. All images were reconstructed at mid-diastole to obtain optimal images of the coronary arteries. In those patients undergoing retrospective electrocardiographically gated scanning, we used a dose modulation protocol to decrease patient exposure to ionizing radiation. The axial image data were reconstructed by using the following parameters: a section thickness of 0.6 mm, an interval of 0.3 mm, a field of view of 24 cm, and a matrix of 512×512. All image analyses were performed using a commercially available workstation (Ziostation2 version 2.9.7.1; AMIN Co., Ltd., Tokyo, Japan; Ziosoft Inc., Tokyo, Japan).

Image Reconstruction and Measurements

The virtual basal ring plane was semi-automatically defined by identifying the nadir of each aortic valvar hingeline, as commonly performed prior to transcatheter aortic valve implantation.[16] Because the virtual basal ring area in mid-diastole usually demonstrates an ellipsoid shape, its dimension was, as usual in clinical practice, represented by the following formula for the circle area equation:

$$Virtual\ basal\ ring_{dimension} = 2 \times \sqrt{\frac{Virtual\ basal\ ring_{area}}{\pi}}.$$

By scrolling up the plane of the virtual basal ring in parallel fashion, the dimension of the sinuses of Valsalva was defined as the bisecting distance from the center of sinus-to-center of opposite interleaflet triangle.[17,18] The dimension of the sinutubular junction was measured as the maximal short-axis distance. It was a plane connecting the apices of the 3 interleaflet triangles, which was commonly not parallel to the plane of the virtual basal ring.[19] The dimensions of the aortic valves were all measured using the 3 center planes bisecting the sinus and opposite interleaflet triangle, which was perpendicular to the virtual basal ring plane (**Figure 1**). Two of three center planes were required to calculate free margin length, by adding each adjoining distance from the tip of interleaflet triangle to the central coaptation of leaflets. In summary, we can obtain 3×2-dimensional values reflecting the dimensions of the sinuses of Valsalva: heights of the interleaflet triangles, geometric height, and free margin length. Effective height and coaptation length were measured using any single plane of these 3 bisecting planes because they are identical using any of these 3 planes (**Figure 1**). **Supplementary Movie** shows a 3-dimensional image of these measurements.

Statistical Analysis

Categorical variables were presented as percentages, whereas continuous variables were presented as mean± standard deviation. The correlation between the continuous variables with normal distribution was evaluated using the Pearson correlation coefficient. Analysis of variance was used to compare continuous variables related to each of the 3 aortic sinuses, leaflets, and interleaflet triangles. For the initial 30 patients, intra-observer and inter-observer reliabilities of geometric height and coaptation length measurements were evaluated by 2 observers with 4 (H.T.) and 8 (Y.I.) years of experience in analysis of cardiac computed tomographic imaging. The intra-observer and inter-observer reliabilities were then assessed using the intra-class correlation coefficient. All statistical analyses were performed using commercially available software (JMP 14.3.0; SAS Institute, Cary, NC, USA). Values of $P<0.05$ were considered statistically significant.

Table 1. Clinical Characteristics of Participants

Variables	n=123
Age (years)	66±12
Men, n (%)	77 (63)
Body height (cm)	162.1±9.9
Body weight (kg)	63.7±15.3
Body mass index (kg/m^2)	24.0±4.4
Body surface area (m^2)	1.69±0.24
Hypertension, n (%)	58 (47)
Dyslipidemia, n (%)	66 (54)
Diabetes mellitus, n (%)	36 (29)
Previous PCI, n (%)	19 (16)
Hemodialysis, n (%)	5 (4)
Indication of CCTA, n (%)	
Atypical chest pain	36 (30)
Pre-/Post-operative assessment	18 (14)
Follow up of coronary artery disease	18 (14)
Abnormal electrocardiogram	15 (12)
Effort angina pectoris	10 (8)
Multiple risk factors	5 (4)
Congenital heart disease	4 (3)
Left ventricular dysfunction	2 (2)
Arrhythmia	2 (2)
Others†	13 (11)
Background cardiac disease, n (%)	
Normal	52 (43)
Ischemic heart disease	48 (39)
Cardiomyopathy	11 (9)
Valvar heart disease	4 (3)
Congenital heart disease	4 (3)
Others‡	4 (3)

†Thirteen cases include cases with syncope, peripheral artery disease, old cerebral infarction, suspected double-chambered right ventricle, coronary artery-pulmonary artery fistula, suspected pericardial tumor, and mild pericardial effusion. ‡Four cases involve cases with paroxysmal atrial fibrillation, pulmonary venous aneurysm, coronary arterial aneurysm, and coronary artery-pulmonary artery fistula. CCTA, coronary arterial computed tomographic angiography; PCI, percutaneous coronary intervention.

Results

The clinical characteristics of participants are presented in **Table 1**. For 123 subjects, the mean age was 66±12 years, with 63% being male. At the time of image acquisition during coronary arterial computed tomographic angiography, the mean heart rate was 64±8 beats/min. Mean reconstruction phase, mean effective radiation doses, and mean contrast material volume were 71±7% of the R–R interval, 3.4±5.5 mSv, and 41±12 mL, respectively.

The dimensions of the aortic root and aortic valve are presented in **Table 2**. The mean dimensions of the virtual basal ring, sinuses of Valsalva, and sinutubular junction were 23.2±2.4, 31.2±3.1, and 27.9±2.8 mm, respectively. The mean ratio between dimensions of the sinutubular junction and virtual basal ring was 1.2±0.1. The mean ratio between dimensions of the sinuses of Valsalva and virtual basal ring was 1.3±0.1. The mean height of the interleaflet triangle was 17.3±1.8 mm. The height of the interleaflet triangle between the non- and left coronary aortic sinuses was significantly shorter than that of the other interleaflet triangles. The mean geometric height was 14.7±1.3 mm. The geometric height of the non-coronary aortic leaflet was the longest, followed by that of the left coronary aortic leaflet and the right coronary aortic leaflet. The effective height and the coaptation length were 8.6±1.4 and 3.2±0.8 mm, respectively. The mean free margin length was 32.6±3.6 mm. The free margin length was longest in the right coronary aortic leaflet and shortest in the left coronary aortic leaflet.

In order to investigate the correlation between the size of the aortic root and aortic leaflets, correlation analysis was performed. The geometric height and the free margin length showed positive correlations with all the measured aortic root dimensions (**Table 3**, **Figure 2**). The effective height showed a positive correlation with the dimensions of the sinuses of Valsalva and sinutubular junction, whereas it was not correlated with the dimension of the virtual basal ring. In contrast, the coaptation length

Table 2. Measured Variables

Variable	n=123		P value (ANOVA)
Aortic root dimension, mm (indexed by body surface area, mm/m^2)			
Virtual basal ring	23.2±2.4	(13.9±1.5)	
Sinuses of Valsalva			<0.0001
Right coronary aortic sinus-to-opposite interleaflet triangle	30.3±3.3*,**		
Left coronary aortic sinus-to-opposite interleaflet triangle	31.1±3.2*,***		
Non-coronary aortic sinus-to-opposite interleaflet triangle	32.3±3.0**,***		
Mean value	31.2±3.1	(18.8±2.5)	
Sinutubular junction	27.9±2.8	(16.8±2.6)	
Virtual basal ring area, mm^2 (indexed by body surface area, mm/m^2)	428.1±87.9	(254.4±40.4)	
Sinutubular junction/Virtual basal ring dimensions ratio	1.2±0.1		
Sinuses of Valsalva/Virtual basal ring dimensions ratio	1.3±0.1		
Height of the interleaflet triangle, mm			<0.0001
Between non- and left coronary aortic sinuses	16.6±2.0*,**		
Between left and right coronary aortic sinuses	17.4±2.2*		
Between right and non-coronary aortic sinuses	17.9±2.5**		
Mean value (indexed by body surface area, mm/m^2)	17.3±1.8	(10.4±1.3)	
Geometric height, mm			<0.0001
Right coronary aortic leaflet	13.9±1.7*,**		
Left coronary aortic leaflet	14.7±1.7*,***		
Non-coronary aortic leaflet	15.3±1.5**,***		
Mean value (indexed by body surface area, mm/m^2)	14.7±1.3	(8.8±1.1)	
Free margin length, mm			<0.0001
Right coronary aortic leaflet	33.9±3.9*,**		
Left coronary aortic leaflet	31.3±3.6*,***		
Non-coronary aortic leaflet	32.7±3.8**,***		
Mean value (indexed by body surface area, mm/m^2)	32.6±3.6	(19.6±2.5)	
Effective height, mm (indexed by body surface area, mm/m^2)	8.6±1.4	(5.2±1.1)	
Coaptation length, mm (indexed by body surface area, mm/m^2)	3.2±0.8	(2.0±0.6)	

*P<0.05 each other. **P<0.05 each other. ***P<0.05 each other. ANOVA, analysis of variance.

showed weak negative correlation with the virtual basal ring, whereas it was not correlated with the dimensions of the sinuses of Valsalva or sinutubular junction (**Table 3**, **Figure 2**).

Excellent intra-observer and inter-observer reliabilities were confirmed for the measurements of the geometric height and coaptation length, as evident in the values of intra-class coefficients of 0.9580 and 0.9499, and 0.9166 and 0.9478, respectively.

Discussion

The aortic root is a complex 3-dimensional structure, composed of the sinuses, leaflets, and interleaflet triangles (**Figures 1**,**3**,**4**, **Supplementary Movie**).[13] Function of the aortic valve depends on the dynamic interaction of aortic leaflets and the other components of the aortic root.[20] Precise preoperative appreciation of the 3-dimensional living anatomy is essential for considering the mechanism of aortic regurgitation to plan adequate aortic valve-sparing surgery.[11,12,14] Several studies have assessed the aortic root geometry by using specimens.[1,21–23] Few studies, however, have revealed the repair-oriented 3-dimensional anatomy of the aortic root using living-heart datasets.[24,25] First, we established the normal standard value and identified individual diversities. Second, correlations between the aortic root size and leaflet measurements were revealed. Regardless of significant variations in the size of the aortic root components, the aortic leaflets display physiological compensation to maintain its constant coaptation.

Asymmetry in Dimensions of the Aortic Sinuses and Leaflets

The aortic sinuses displays subtle asymmetry in size, with the right and non-coronary aortic sinuses being the largest, the left coronary aortic sinus being the smallest, and the leaflet sizes mirroring their respective sinuses.[20,23–26] Our findings of the longest and shortest free margin length of the right and left coronary aortic leaflets, respectively, was consistent with previous studies.[20,23] This anatomical asymmetry reflect the stress applied to the aortic sinuses, which is also asymmetric.[27,28]

Even though both free margin length and geometric height seem to reflect the size of the leaflet, the geometric height of the right coronary aortic leaflet was paradoxically shorter than the other aortic leaflets. This may reflect the characteristic anatomical relationship between the virtual basal ring and sinuses of Valsalva (**Figure 3**). The bisecting cut through the right coronary aortic sinus is nearly equal to the short axis of the ellipsoid virtual basal ring,[19] depending on the degree of rotation of the aortic root.[29] Accordingly, the distance from the nadir of the hingelines to the central coaptation zone should be shortest in the right coronary aortic sinus (**Figure 3**). In other words, the

Table 3. Analysis of the Correlation of Aortic Valve Dimensions

Variable	Geometric height			Free margin length		
	β	r^2	P value	β	r^2	P value
Age	−0.0382	0.1183	<0.0001	−0.0283	0.0089	0.3000
Sex (men)	0.5749	0.3305	<0.0001	0.6101	0.3723	<0.0001
Body height	0.0794	0.3493	<0.0001	0.2084	0.3279	<0.0001
Body weight	0.0422	0.2348	<0.0001	0.0940	0.1586	<0.0001
Body mass index	0.0784	0.0662	0.0041	0.1406	0.0291	0.0594
Body surface area	3.0805	0.2997	<0.0001	7.2936	0.2293	<0.0001
Aortic root dimension						
Virtual basal ring	0.3891	0.4865	<0.0001	1.0618	0.4944	<0.0001
Sinuses of Valsalva	0.2924	0.4574	<0.0001	0.9021	0.5940	<0.0001
Sinutubular junction	0.2298	0.2397	<0.0001	0.8400	0.4372	<0.0001
Height of the interleaflet triangle	0.5023	0.4882	<0.0001	1.6985	0.7617	<0.0001
Geometric height				1.5208	0.3156	<0.0001
Free margin length	0.2075	0.3156	<0.0001			
Effective height	0.5598	0.3259	<0.0001	0.1118	0.0018	0.6438
Coaptation length	0.5046	0.0860	0.0010	−0.9397	0.0407	0.0253
	Effective height			**Coaptation length**		
	β	r^2	P value	β	r^2	P value
Age	0.0023	0.0004	0.8205	−0.0037	0.0032	0.5318
Sex (men)	0.2059	0.0424	0.0223	−0.1308	0.0171	0.1493
Body height	0.0274	0.0400	0.0266	−0.0092	0.0138	0.1949
Body weight	0.0080	0.0080	0.3251	−0.0021	0.0018	0.6413
Body mass index	−0.0032	0.0001	0.9102	0.0024	0.0002	0.8804
Body surface area	0.6898	0.0144	0.1854	−0.2204	0.0045	0.4588
Aortic root dimension						
Virtual basal ring	0.0522	0.0084	0.3129	−0.0686	0.0447	0.0189
Sinuses of Valsalva	0.2047	0.2155	<0.0001	−0.0292	0.0135	0.2007
Sinutubular junction	0.2100	0.1925	<0.0001	−0.0226	0.0069	0.3618
Height of the interleaflet triangle	0.2421	0.1090	0.0002	−0.0031	0.0001	0.9353
Geometric height	0.5822	0.3259	<0.0001	0.1704	0.0860	0.0010
Free margin length	0.0159	0.0018	0.6438	−0.0433	0.0407	0.0253
Effective height				0.2562	0.2021	<0.0001
Coaptation length	0.7890	0.2021	<0.0001			

right coronary aortic leaflet does not require a long geometric height to achieve the same effective height, even though its free margin length is the longest, reflecting the largest size of the sinus.

Comparison With Previous Findings

Intraoperative direct measurements from the patients undergoing aortic valve repair procedures reported that mean geometric heights in those with a mean body surface area of 2.0 m^2 was approximately 20 mm.[22] The value was greater than the present value of 14.7 mm, which was measured by computed tomography using a smaller Japanese population (mean body surface area of 1.7 m^2) that had no pathological aortic roots. The present mean value of the free margin length (32.6 mm) is compatible with that obtained from aortic homografts (34.3 mm).[23] In normal aortic valves, the effective height ranges from 8 to 10 mm.[2] An effective height <8 mm in the presence of normal geometric height is an indicator of prolapse.[11] Our present data with a mean effective height of 8.6 mm support this statement. Coaptation height was only 3.2 mm, which is also consistent with that obtained from aortic homografts (3.3 mm).[23]

Limitations of 2-Dimensional Evaluation

Dimensions of the virtual basal ring and the sinuses of Valsalva varied between the various modalities and methodologies due to the complex shape of the aortic root.[19] Precise measurement of the aortic valve requires dedicated 3-dimensional bisecting planes orthogonal to the virtual basal ring (**Figure 1**).[12,19] Precise measurement of the geometric height requires both nadir of the hingeline and central zone of coaptation. Without projecting the virtual basal ring to the orthogonal plane cut through the central zone of coaptation, the precise effective height cannot be measured. Coaptation length can be overestimated when using the off-center cut (**Figure 3**). As any of these values are clinically important for both preoperative planning and postoperative evaluation,[30,31] it is time to revisit these values with reference to 3-dimensional evaluation. In addition to the advantage of 3-dimensional echocardiography to provide real-time dynamic information,[14] preoperative computed tomographic data will provide complementary information with its excellent spatial resolution with a wide field of view. These 3-dimensional quantitative techniques will further sophisticate current valve-sparing surgery towards a more patient-specific approach.

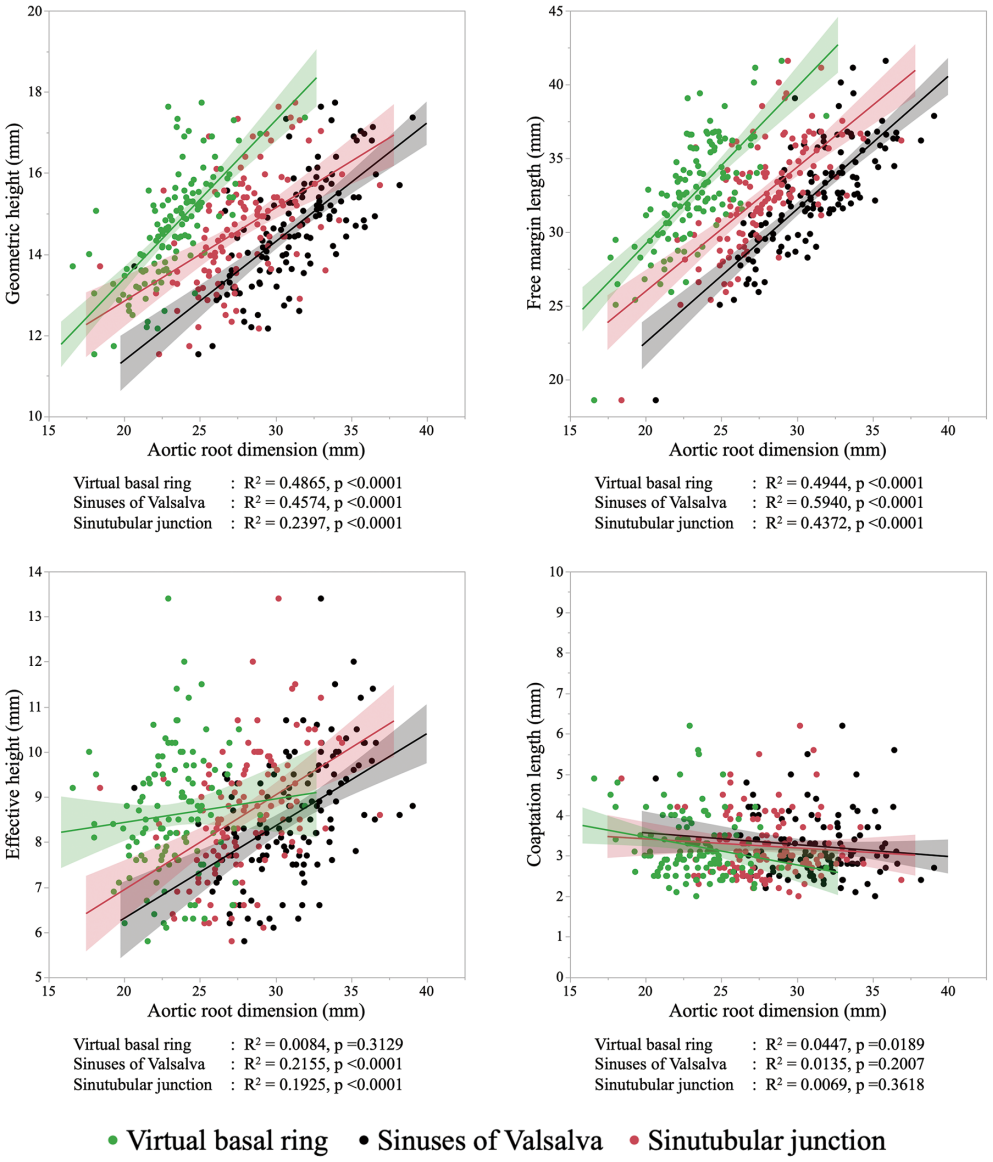

Figure 2. Relationships between the dimensions of the aortic root and the aortic leaflet measurements.

Clinical Implications

The geometric height and free margin length can now be measured in a non-invasive preprocedural fashion with the patient in their natural hemodynamic state. These 2 values would be constant unless valvuloplasty is performed. This can preclude the potential limitation of intraoperative measurements of the bloodless heart under extracorporeal support. If we compare preoperative values of dysfunctional aortic valves to current physiologic values from normal cases, the differences can then provide a clue for precise evaluation of etiology and guide the effective repair strategy.

Although computed tomographic measurement can provide reproducible values in a physiological state with its high spatial resolution, cardiac surgeons should keep in mind discrepancies between preoperative computed tomographic measurements and intraoperative measurements, especially for the geometric height.[32] Komiya et al demonstrated that the intraoperative measurement value of geometric height was, on average, 1.7 mm larger than the preoperative computed tomographic measurement.[32] This small difference matters because the precise measurement of the leaflet size represented by the geometric height is important to avoid aortic root-leaflet mismatch (relative shortage of geometric height leading to a coaptation length <2 mm) to secure appropriate coaptation.[32] Overestimation of leaflet size has a risk to trigger insufficient annuloplasty, which leads to residual aortic regurgitation due to inappropriate coaptation.

It has been reported that low effective height (<9 mm) and short coaptation length (<4 mm) lead to postoperative aortic valve regurgitation in aortic valvuloplasty.[30,31,33] These postoperative values seem larger than current

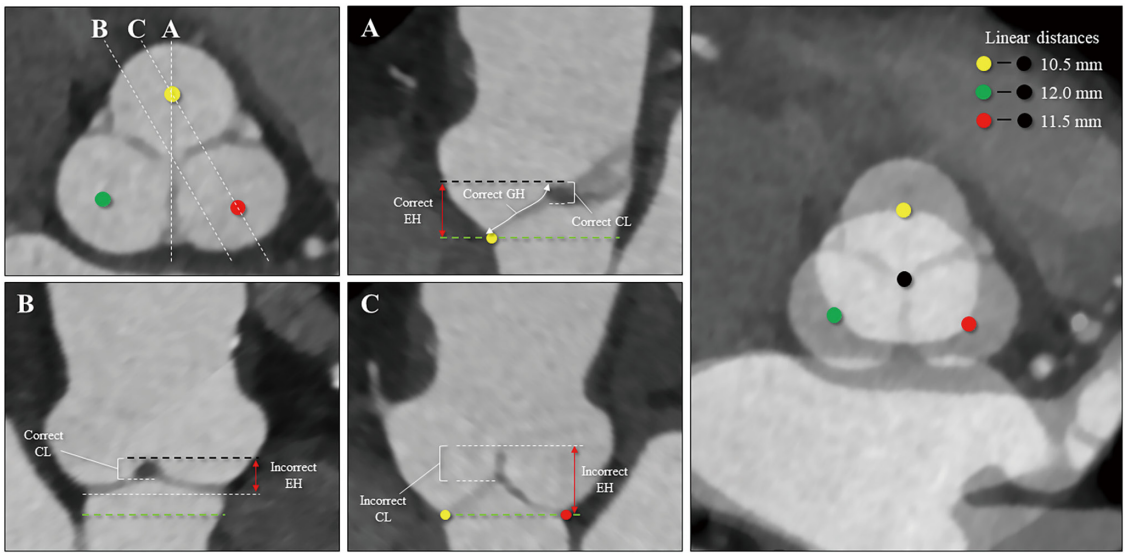

Figure 3. Difference in appearance of the effective height and coaptation length among each longitudinal section orthogonal to the virtual basal ring. The left upper panel is the reference section at the level of sinuses of Valsalva parallel to the virtual basal ring. Sections indicated by white dashed lines (**A**–**C**) correspond to the sections presented in the following panels. (**A**) Bisecting plane (center of sinus-to-center of interleaflet triangle). This plane can demonstrate the correct geometric height, effective height (if the virtual basal ring plane is adequately projected), and coaptation length. (**B**) Longitudinal center plane so as to visualize the aortic sinuses symmetrically. This plane cannot show the correct geometric height and effective height as this cannot provide the virtual basal ring plane. Coaptation length is correct as this is the center plane. (**C**) Largest sinus-to-sinus plane. When this section is cut through the 2 adjacent nadirs of the hingelines, it can provide the virtual basal ring plane. However, this plane overestimates the effective height and coaptation length as the central zone of coaptation is lower than the plane of sinutubular junction, and the coaptation surface area increases when moving away from the central point towards the "commissures", respectively. Geometric height is not correct as this plane is out of the central zone of coaptation. Thee yellow-green dashed line represents the virtual basal ring plane. The right hand panel shows the location of the ellipsoid virtual basal ring superimposed on a section of the sinuses of Valsalva. This image can explain the reason why the geometric height of the right coronary aortic sinus is the shortest. Yellow, red, and green circles indicate the 3 nadirs of the hingelines of the right, left, and non-coronary aortic leaflets, respectively. The black circle indicates the nodule of Arantius. CL, coaptation length; EH, effective height; GH, geometric height.

preoperative values. This discrepancy may reflect that the clinical goal of the aortic valve-sparing surgery is not simply restoring normal anatomy but optimizing the physiological function of the aortic valve with some safety margin.[32] Even applying a 4–6 mm safety margin to ensure sufficient coaptation, this is narrower than that of the mitral valve. Consequently, aortic valve-sparing surgery requires experience, expertise, and more sophisticated tools,[32] which makes the standardization of this procedure difficult. However, any of previous 2-dimensional measurements should be evaluated carefully, as they can show potential inaccuracy (**Figure 3**).[11,18] Further investigation is required to revisit postoperative values with 3-dimensional methods in relation to clinical outcomes.

In selecting graft size, measuring the dimensions of the ventriculo-aortic and sinutubular junctions,[34] and the height of the interleaflet triangle[35] have been proposed in aortic valve-sparing surgery. Komiya et al demonstrated a prediction model using mathematical calculations to optimize annuloplasty from the given geometric height.[32] In the model, effective height was preset at 8 mm. The model provides a reasonable and practical value of the annulus diameter for annuloplasty to achieve the target coaptation length. As their model showed,[32] the present data (**Table 3**, **Figure 2**) obtained from patients with normal aortic valves by direct measurement confirmed a positive correlation between leaflet size and aortic root dimensions to secure the effective height[2] and to maintain optimal and constant coaptation.[36,37]

The diameter of the sinutubular junction is approximately 1.2-fold larger than that of the virtual basal ring when evaluated by transthoracic echocardiography.[30] This relationship was confirmed by the present analysis using 3-dimensional computed tomographic measurement with more precision (**Table 2**). As the aortic leaflets are supported by the entire aortic root, focusing on every dimension involving the virtual basal ring, sinuses of Valsalva, and sinutubular junction is increasingly important to perform optimal valve-sparing surgery. In this regard, Zakkar et al recently published the clinical superiority of double ring annuloplasty performed using an external ring at the conventional subvalvar level and additional sinutubular junction level.[38] This concept suggests an importance to optimize the entire size of the aortic root relative to each leaflet size to avoid aortic root–leaflet size mismatch.

Finally, this study implies potential utility of preoperative cardiac computed tomography for detailed assessment of aortic valve and aortic root in patients with aortic regurgitation.

Study Limitations

First, a single-center retrospective design cannot eliminate

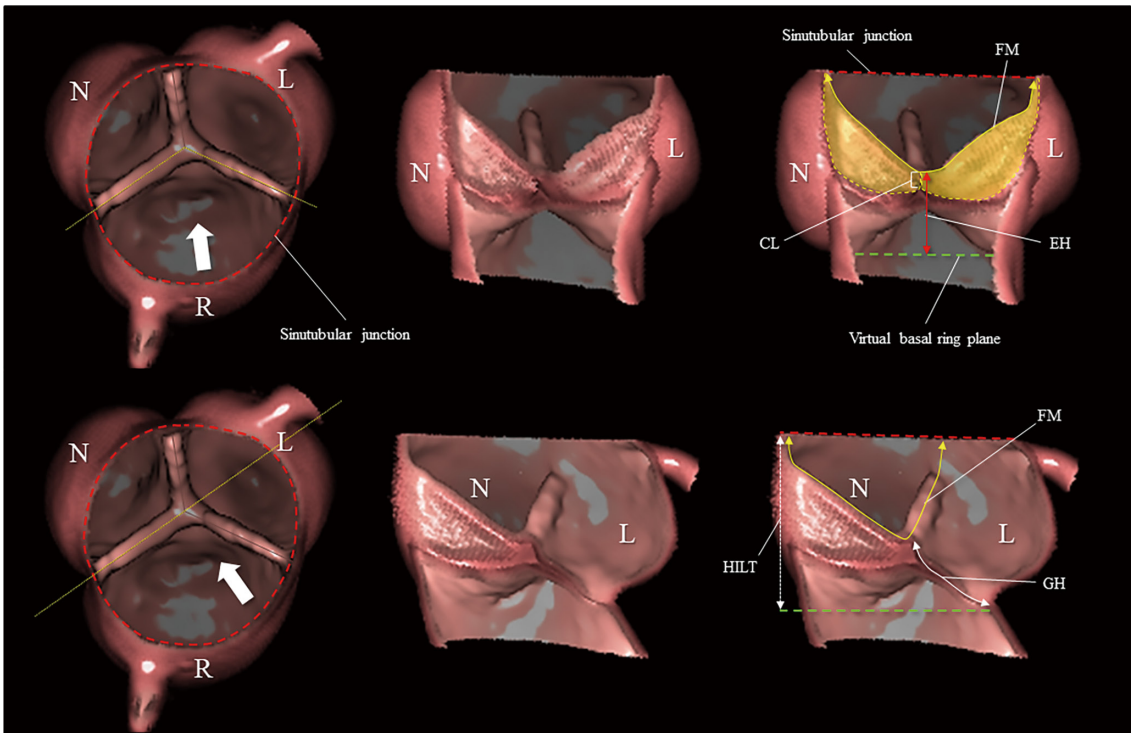

Figure 4. Volume-rendering images of the aortic root and valve. Yellow dotted lines in the left panels indicate the sectional direction shown in the center and right panels. White arrows in the left panels denote the view of direction for the center and right panels. Yellow-green and red dashed lines represent the virtual basal ring and sinutubular junction planes, respectively. White dashed double-head arrow represents the height of the interleaflet triangle. White solid double-head arrows indicate the geometric height. Yellow double-head arrows denote free margin lengths. The effective height (red double-head arrow) represents the vertical distance between the virtual basal ring and the top of the central zone of coaptation. The coaptation length was defined as the distance of central coaptation of the leaflets. The yellow zone in the right superior panel marks the zones of coaptation, showing the reason why the effective height and coaptation length should be measured at the central zone of coaptation. CL, coaptation length; EH, effective height; FM, free margin; GH, geometric height; HILT, height of the interleaflet triangle; L, left coronary aortic sinus; N, non-coronary aortic sinus; R, right coronary aortic sinus.

selection bias, and causal relationships are difficult to be proven as well. Even if patient records showed any background cardiac diseases, including cardiomyopathy, valvar heart disease, and congenital heart disease, those patients were enrolled in the current analysis (**Table 1**) unless the diagnoses had hemodynamic or structural significance to patients, and unless they showed functional or structural abnormality of the aortic valve and aortic root. Nevertheless, the average values of key measurements were identical between those cases with background cardiac diseases and those without (**Supplementary Table**). Second, as mid-diastolic images were used, a dynamic change of the aortic root geometry could not be investigated. Third, our results were obtained from patients without aortic valvar and ascending aortic diseases. However, the normal anatomy should be investigated at first so as to create normative values. Finally, the present study was composed of a Japanese population with a mean body surface area of $1.69\pm0.24\,m^2$. The index value provided in **Table 1**, however, would retain its clinical importance for non-Asian populations.

Conclusions

Normal adult dimensions of the aortic valve were demonstrated using living-heart datasets. Regardless of significant variations in the size of the aortic root, the aortic valve shows physiological compensation to maintain its optimal coaptation. These measurements will serve as the standard value for preoperative evaluation of the aortic valvar anatomy, to plan optimal aortic valve-sparing surgery.

Acknowledgments

The authors thank Dr. Masataka Suzuki, Dr. Yu Takahashi, Dr. Daisuke Tsuda, Dr. Shinsuke Shimoyama, and Dr. Sei Fujiwara for their cooperation in the acquisition and reconstruction of the images, which could not have been produced without the technical support provided by our radiological technologists: Takuro Nishio, Tomoki Maebayashi, Wakiko Tani, Kiyosumi Kagawa, and Noriyuki Negi.

Disclosures

K.H. is a member of *Circulation Journal*' Editorial Team.

IRB Information

The ethics committee from Kobe University Hospital Clinical Translational Research Center (ref no. 180242) approved this study.

Data Availability

The deidentified participant data will not be shared.

References

1. De Kerchove L, Jashari R, Boodhwani M, Duy KT, Lengelé B, Gianello P, et al. Surgical anatomy of the aortic root: Implication for valve-sparing reimplantation and aortic valve annuloplasty. *J Thorac Cardiovasc Surg* 2015; **149:** 425–433.
2. Schäfers HJ, Bierbach B, Aicher D. A new approach to the assessment of aortic cusp geometry. *J Thorac Cardiovasc Surg* 2006; **132:** 436–438.
3. Khelil N, Sleilaty G, Palladino M, Fouda M, Escande R, Debauchez M, et al. Surgical anatomy of the aortic annulus: Landmarks for external annuloplasty in aortic valve repair. *Ann Thorac Surg* 2015; **99:** 1220–1226.
4. David TE. Additional anatomic information on the aortic root. *J Thorac Cardiovasc Surg* 2015; **149:** 408–410.
5. Tretter JT, Spicer DE, Mori S, Chikkabyrappa S, Redington AN, Anderson RH. The significance of the interleaflet triangles in determining the morphology of congenitally abnormal aortic valves: Implications for noninvasive imaging and surgical management. *J Am Soc Echocardiogr* 2016; **29:** 1131–1143.
6. David TE, Maganti M, Armstrong S. Aortic root aneurysm: Principles of repair and long-term follow-up. *J Thorac Cardiovasc Surg* 2010; **140:** S14–S19.
7. David TE, Armstrong S, Manlhiot C, McCrindle BW, Feindel CM. Long-term results of aortic root repair using the reimplantation technique. *J Thorac Cardiovasc Surg* 2013; **145:** S22–S25.
8. Coselli JS, Volguina IV, LeMaire SA, Sundt TM, Connolly HM, Stephens EH, et al. Early and 1-year outcomes of aortic root surgery in patients with Marfan syndrome: A prospective, multicenter, comparative study. *J Thorac Cardiovasc Surg* 2014; **147:** 1758–1766, 1767.e1–1767.e4.
9. Oka T, Okita Y, Matsumori M, Okada K, Minami H, Munakata H, et al. Aortic regurgitation after valve-sparing aortic root replacement: Modes of failure. *Ann Thorac Surg* 2011; **92:** 1639–1644.
10. Stephens EH, Liang DH, Kvitting JP, Kari FA, Fischbein MP, Mitchell RS, et al. Incidence and progression of mild aortic regurgitation after Tirone David reimplantation valve-sparing aortic root replacement. *J Thorac Cardiovasc Surg* 2014; **147:** 169–177, 178.e1–178.e3.
11. Schäfers HJ. The 10 commandments for aortic valve repair. *Innovations (Phila)* 2019; **14:** 188–198.
12. Mori S, Izawa Y, Shimoyama S, Tretter JT. Three-dimensional understanding of complexity of the aortic root anatomy as the basis of routine two-dimensional echocardiographic measurements. *Circ J* 2019; **83:** 2320–2323.
13. Tretter JT, Mori S. Two-dimensional imaging of a complex three-dimensional structure: Measurements of the aortic root dimensions. *J Am Soc Echocardiogr* 2019; **32:** 792–794.
14. Hagendorff A, Evangelista A, Fehske W, Schäfers HJ. Improvement in the assessment of aortic valve and aortic aneurysm repair by 3-dimensional echocardiography. *JACC Cardiovasc Imaging* 2019; **12:** 2225–2244.
15. Mori S, Spicer DE, Anderson RH. Revisiting the anatomy of the living heart. *Circ J* 2016; **80:** 24–33.
16. Kasel AM, Cassese S, Bleiziffer S, Amaki M, Hahn RT, Kastrati A, et al. Standardized imaging for aortic annular sizing: Implications for transcatheter valve selection. *JACC Cardiovasc Imaging* 2013; **6:** 249–262.
17. Suzuki M, Mori S, Izawa Y, Shimoyama S, Takahashi Y, Toh H, et al. Three-dimensional volumetric measurement of the aortic root compared to standard two-dimensional measurements using cardiac computed tomography. *Clin Anat*, doi:10.1002/ca.23597.
18. Toh H, Mori S, Tretter JT, Izawa Y, Shimoyama S, Suzuki M, et al. Living anatomy of the ventricular myocardial crescents supporting the coronary aortic sinuses. *Semin Thorac Cardiovasc Surg* 2020; **32:** 230–241.
19. Mori S, Anderson RH, Tahara N, Izawa Y, Toba T, Fujiwara S, et al. The differences between bisecting and off-center cuts of the aortic root: The three-dimensional anatomy of the aortic root reconstructed from the living heart. *Echocardiography* 2017; **34:** 453–461.
20. Kunzelman KS, Grande KJ, David TE, Cochran RP, Verrier ED. Aortic root and valve relationships. Impact on surgical repair. *J Thorac Cardiovasc Surg* 1994; **107:** 162–170.
21. Silver MA, Roberts WC. Detailed anatomy of the normally functioning aortic valve in hearts of normal and increased weight. *Am J Cardiol* 1985; **55:** 454–461.
22. Schäfers HJ, Schmied W, Marom G, Aicher D. Cusp height in aortic valves. *J Thorac Cardiovasc Sur* 2013; **146:** 269–274.
23. De Kerchove L, Momeni M, Aphram G, Watremez C, Bollen X, Jashari R, et al. Free margin length and coaptation surface area in normal tricuspid aortic valve: An anatomical study. *Eur J Cardiothorac Surg* 2018; **53:** 1040–1048.
24. Gooley RP, Cameron JD, Soon J, Loi D, Chitale G, Syeda R, et al. Quantification of normative ranges and baseline predictors of aortoventricular interface dimensions using multi-detector computed tomographic imaging in patients without aortic valve disease. *Eur J Radiol* 2015; **84:** 1737–1744.
25. Yang DH, Kim DH, Handschumacher MD, Levine RA, Kim JB, Sun BJ, et al. In vivo assessment of aortic root geometry in normal controls using 3D analysis of computed tomography. *Eur Heart J Cardiovasc Imaging* 2017; **18:** 780–786.
26. Vollebergh FE, Becker AE. Minor congenital variations of cusp size in tricuspid aortic valves: Possible link with isolated aortic stenosis. *Br Heart J* 1977; **39:** 1006–1011.
27. Grande KJ, Cochran RP, Reinhall PG, Kunzelman KS. Stress variations in the human aortic root and valve: The role of anatomic asymmetry. *Ann Biomed Eng* 1998; **26:** 534–545.
28. Lansac E, Lim HS, Shomura Y, Lim KH, Rice NT, Goetz WA, et al. Aortic root dynamics are asymmetric. *J Heart Valve Dis* 2005; **14:** 400–407.
29. Tretter JT, Mori S, Saremi F, Chikkabyrappa S, Thomas K, Bu F, et al. Variations in rotation of the aortic root and membranous septum with implications for transcatheter valve implantation. *Heart* 2018; **104:** 999–1005.
30. Bierbach BO, Aicher D, Issa OA, Bomberg H, Gräber S, Glombitza P, et al. Aortic root and cusp configuration determine aortic valve function. *Eur J Cardiothorac Surg* 2010; **38:** 400–406.
31. Kunihara T, Aicher D, Rodionycheva S, Groesdonk HV, Langer F, Sata F, et al. Preoperative aortic root geometry and postoperative cusp configuration primarily determine long-term outcome after valve-preserving aortic root repair. *J Thorac Cardiovasc Surg* 2012; **143:** 1389–1395.
32. Komiya T, Shimamoto T, Nonaka M, Matsuo T. Is small cusp size a limitation for aortic valve repair? *Eur J Cardiothorac Surg* 2019; **56:** 497–502.
33. le Polain de Waroux JB, Pouleur AC, Robert A, Pasquet A, Gerber BL, Noirhomme P, et al. Mechanisms of recurrent aortic regurgitation after aortic valve repair: Predictive value of intraoperative transesophageal echocardiography. *JACC Cardiovasc Imaging* 2009; **2:** 931–939.
34. Doty DB, Arcidi JM. Methods for graft size selection in aortic valve-sparing operations. *Ann Thorac Surg* 2000; **69:** 648–650.
35. De Kerchove L, Boodhwani M, Glineur D, Noirhomme P, El Khoury G. A new simple and objective method for graft sizing in valve-sparing root replacement using the reimplantation technique. *Ann Thorac Surg* 2011; **92:** 749–751.
36. Mangini A, Lemma MG, Soncini M, Votta E, Contino M, Vismara R, et al. The aortic interleaflet triangles annuloplasty: A multidisciplinary appraisal. *Eur J Cardiothorac Surg* 2011; **40:** 851–857.
37. Lansac E, Di Centa I, Sleilaty G, Crozat EA, Bouchot O, Hacini R, et al. An aortic ring: From physiologic reconstruction of the root to a standardized approach for aortic valve repair. *J Thorac Cardiovasc Surg* 2010; **140:** S28–S35; discussion S45–S51.
38. Zakkar M, Bruno VD, Zacek P, Di Centa I, Acar C, Khelil N, et al. Isolated aortic insufficiency valve repair with external ring annuloplasty: A standardized approach. *Eur J Cardiothorac Surg* 2020; **57:** 308–316.

Supplementary Files

Supplementary Movie. Three-dimensional image to show the concept of precise measurements of the complicated anatomy of the aortic leaflets. Red, yellow, white, and yellow-green lines indicate the sinutubular junction, free margin, geometric heights, and virtual basal ring, respectively. CRA, cranial; LAO, left anterior oblique; RAO, right anterior oblique.

Please find supplementary file(s);
http://dx.doi.org/10.1253/circj.CJ-20-0938